Proceedings of the 9th U.S. National and 10th Canadian Conference on Earthquake Engineering
Compte Rendu de la 9ième Conférence Nationale Américaine et
10ième Conférence Canadienne de Génie Parasismique
July 25-29, 2010, Toronto, Ontario, Canada • Paper No 701

SEISMIC PERFORMANCE OF HIGH-STRENGTH-CONCRETE HOLLOW BRIDGE PIERS UNDER MULTI-DIRECTIONAL LOADING

R. Burgueño[1], X. Liu[2] and E. M. Hines[3]

ABSTRACT

High-strength-concrete (HSC) offers the potential of transforming seismic design concepts by harnessing the enhanced capacities associated with axial load, flexural compression zone confinement and web shear crushing of wall webs. Recent research has demonstrated that structural walls can exhibit dependable ductile behavior before being ultimately limited by web crushing shear failures and that this inelastic capacity can be further improved with HSC. The performance of hollow square HSC bridge piers under multi-directional was thus evaluated to help define limits that satisfy the noted performance requirements. Two 1/4-scale units, with design concrete compressive strengths of 34 and 138 MPa (5 and 20 ksi), were subjected to diagonal and multi-directional cyclic loading, respectively. The 3D inelastic web crushing behavior and the degradation of shear stiffness and energy dissipating capacity was evaluated. Results indicate that the mixed flexure-shear cracking mode under multi-directional loading causes rapid shear stiffness degradation and accelerates the subsequent web crushing failure.

Introduction

High-strength-concrete (HSC) offers the potential of transforming the design of structural elements under seismic loads by harnessing the enhanced capacities associated with axial load, flexural compression zone confinement and web shear crushing of wall webs. Recent research (Liu 2009) has expanded prior evidence to demonstrate that pier walls under shear demands considerably above current design limits can exhibit stable ductile behavior before experiencing web crushing shear failures; and that their inelastic deformation capacity can be further improved by using high-strength-concrete (HSC). Such facts thus lead to the suggestion that inelastic flexure-shear behavior with subsequent inelastic shear failure can satisfy seismic performance requirements on bridge piers.

[1]Associate Professor, Dept. of Civil and Environmental Eng., Michigan State University, East Lansing, MI 48824
[2]Graduate Assistant, Dept. of Civil and Environmental Eng., Michigan State University, East Lansing, MI 48824
[3]Professor of Practice, Dept. of Civil and Environmental Eng., Tufts University, Medford, MA 02155

Of the noted aspects enhanced by HSC, that associated with the inelastic web crushing capacity of hollow rectangular bridge piers remains unresolved in view of the guidance of capacity design philosophy which suppresses possible shear failures. Several issues are addressed as follows. First, the limits to which such performance features can be reliably taken into account require careful exploration. Second, the three-dimensional demand and web crushing capacity of HSC bridge piers under multi-directional loading needs to be properly evaluated in order to establish reliable limits that satisfy the noted inelastic performance requirements. Third, the use of HSC entails careful damage assessment to meet serviceability objectives and explicit criteria on performance limits to ensure meeting safety.

The vulnerability of bridges subjected to earthquake motions along random directions makes the performance evaluation of piers under multi-directional loading necessary. Although noteworthy research has been done on the behavior of hollow bridge piers under biaxial loading, most of it was focused on assessing biaxial flexural behavior and slenderness limits (Maria 2006). Mo *et al* (Mo 2003) studied the seismic performance of hollow bridge columns under uni-directional cyclic loading. Takizawa *et al* (Takizawa 1976) and Bousias *et al* (Bousias 1995) studied the biaxial flexural behavior of pier columns under various loading patterns with the aim of establishing the interaction, or coupling, effects between the two perpendicular directions. Hines *et al*. (Hines 2006) conducted two proof-of-concept tests on a typical hollow rectangular skyway pier of the new San Francisco-Oakland Bay Bridge (SFOBB), which focused on evaluating a pier design with highly-reinforced boundary elements and connecting walls subjected to uni-directional and bi-directional cyclic loading.

All of the above-noted efforts were related to the flexural behavior of the hollow rectangular piers and none has considered shear demands and failure modes under multi-directional loading. A related investigation related to shear behavior is the work by Wong *et al.* (Wong 1993) who studied the ductility level and different failure modes of circular columns with an aspect ratio of 2. Test results revealed that biaxial displacement patterns led to severe strength and stiffness degradation compared to uniaxial displacement and that shear failures with moderate ductility could be achieved. Thus, even though the mechanisms behind inelastic plane shear web crushing has been reported for some time (Oesterle 1979, Vallenas 1979, Hines 2004) the three-dimensional shear resistance and failure mechanism of hollow rectangular bridge piers is still not fully investigated.

To address the knowledge gap and evaluate the potential of HSC to allow for ductile shear failures as an acceptable inelastic failure mechanism, two 1/4-scale hollow rectangular bridge piers subjected to multi-directional cyclic loading with design concrete strengths of 34 and 138 MPa (5 and 20 ksi) were tested. The three-dimensional inelastic web crushing behavior was evaluated from observations and measured hysteretic force-displacement behavior. Loading path effects on web crushing capacity and the degradation of shear stiffness and energy dissipating capacity were quantified. Test results support that HSC can delay web crushing shear failures, thus allowing for the dependable inelastic response of hollow bridge piers. However, the mixed flexure-shear cracking mode under multi-directional loading causes rapid shear stiffness degradation, an effect that is amplified for HSC due to its lower fracture toughness.

Experimental Investigation

To verify the above-noted hypothesis and establish rational performance levels on the inelastic web crushing limits for HSC pier walls, two bridge piers were constructed and tested at the NEES MAST laboratory at the University of Minnesota (Liu 2009). The 34 MPa (5 ksi) pier, identified as the diagonal pier test (DPT) unit, was subjected to a standard, incrementally increasing, fully-reversed cyclic pattern, with constant axial load increasing about the section's diagonal axis with two cycles at each ductility level. The 138 MPa (20 ksi) pier, identified as biaxial pier test (BPT) unit, was loaded using the biaxial loading protocol proposed by Hines *et al* (Hines 2006) which subjected the pier to deformations along their principal and diagonal (bi-directional) axes and in a sweeping motion from one principal axis to another. The loading protocol was developed based on non-linear time-history analyses of the SFOBB Skyway for six different earthquake time histories. The biaxial loading protocol allows for comparison of damage and performance at specified displacement ductility levels for four major axes of rotation. The loading patterns for both DPT and BPT are shown in Fig. 1. For both tests, displacement ductility was regularly increased according to the sequence of 1, 1.5, 2, 3, 4 and 6.

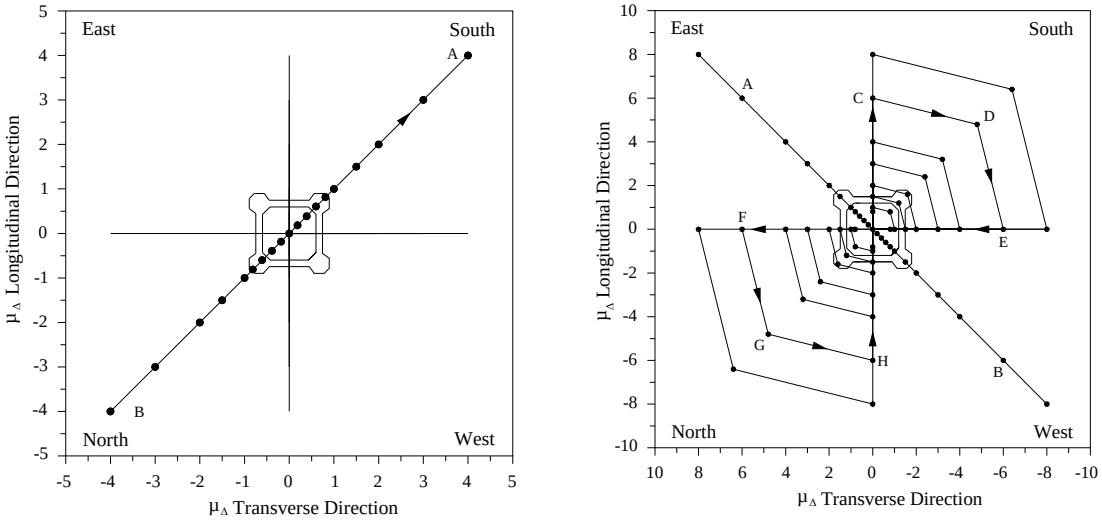

Figure 1. (a) DPT diagonal loading protocol; and (b) BPT biaxial loading protocol.

An elevation of the pier test units and the cross section and reinforcement details of the DPT test unit are shown in Fig. 2 and 3. The overall dimensions of the test units were dictated by construction and test setup constraints. The test unit featured highly-reinforced and well-confined boundary corner elements with thin connecting walls arranged symmetrically in the form of a hollow square. The concrete confining effect of the boundary elements was provided by a steel spiral, the interval of which was 50 mm (2 in.) within the plastic hinge length and 76 mm (3 in.) outside of it. Both test units shared the same cross-sectional geometrical dimensions as well as the longitudinal and confining steel configurations. Other than the concrete compressive strength the only difference between the test units was on the vertical spacing of the wall transverse steel. The DPT unit had its wall transverse steel uniformly distributed at 102 mm (4 in.) along the height, while the spacing was 76 mm (3 in.) for the BPT unit in order to provide greater diagonal tension resistance under shear.

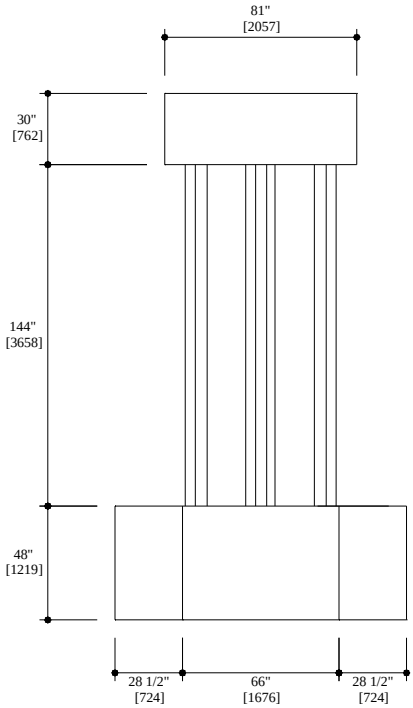

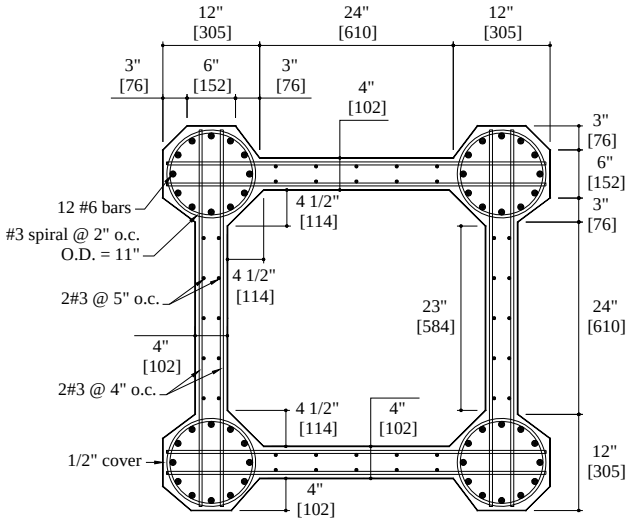

Figure 2. Elevation of the pier test units (Left).

Figure 3. Cross section of DPT unit with reinforcement details (Above).

Fig. 4 shows an overview test setup at the MAST laboratory at the University of Minnesota. The MAST facility operates by controlling the six degrees of freedom of a stiff crossbeam, to which the test unit is attached, by means of eight servo-controlled actuators (two under each principal horizontal direction and four vertical actuators at the ends of the crossbeam. A flexure/shear aspect ratio of 2.5 was maintained by controlling the loading such as to create an inflection point 3 m (120 in.) above the top of the footing (Fig. 5). All displacement related results and parameters (e.g., displacement ductility) reported in the next sections are with respect to the measured lateral deformations at the inflection point. Both units were tested under a constant axial load of 434 kips, corresponding to $0.10f'_cA_g$ for the 34 MPa (5 ksi) test unit.

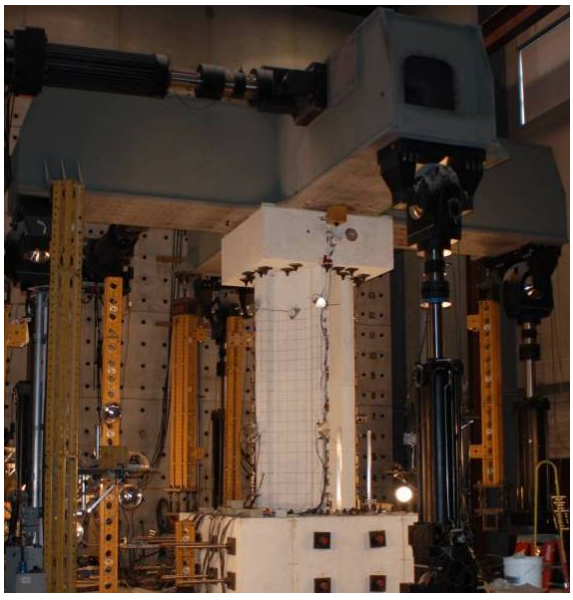

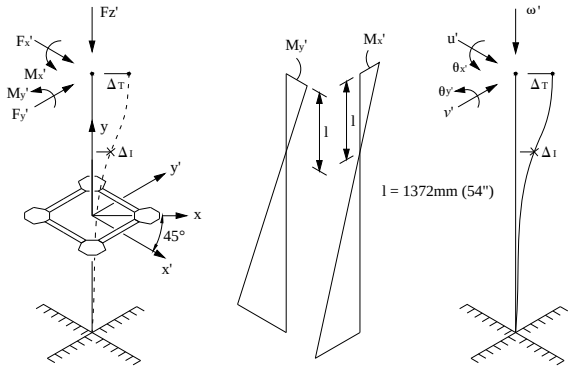

Figure 4. BPT test setup overview (Left).

Figure 5. Loading components and moment diagram (Above).

Experimental Results

Both pier test units behave in a ductile manner before web crushing failure accompanied by the spalling of wall concrete and gradual loss of load-carrying capacity. The DPT unit failed on the second excursion to point A at displacement ductility (μ_Δ) 4 and the BPT unit failed on the excursion to point B at $\mu_\Delta = 6$ (see Fig. 1). Figure 6 shows the cracking pattern and the web crushing failure mode of DPT unit. The flexural demands on the pier led to concrete spalling on compression boundary elements and the NE wall, which mainly concentrated at the bottom of the specimen. The inelastic flexure-shear cracking effects can be observed on all walls and the critical damage and concrete spalling in the SW wall led to the ultimate failure of the test unit. The gradual loss of the load-carrying capacity demonstrated a ductile web crushing failure.

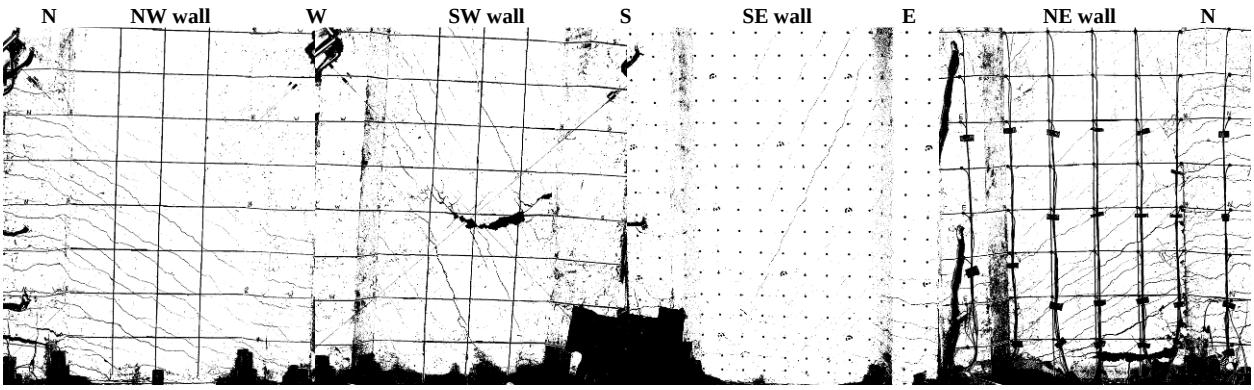

Figure 6. DPT web crushing failure at $\mu_\Delta = 4$ x 2 loading toward A.

Figure 7 shows the cracking pattern and the web crushing failure mode of BPT unit. Web crushing on this unit took place initiated at the region next to the compression boundary element, which was severely degraded due to the multi-directional loading demands. The failure, however, was limited to the plastic hinge region of the walls. Spalling of the wall cover concrete was observed on NW side at the interface of the wall and boundary element. Ultimate failure of the test unit was due to rupture of the transverse reinforcement immediately above the critical section and subsequent longitudinal bar buckling on the compression boundary element when loading toward A at $\mu_\Delta = 8$ upon completing a full cycle at $\mu_\Delta = 6$.

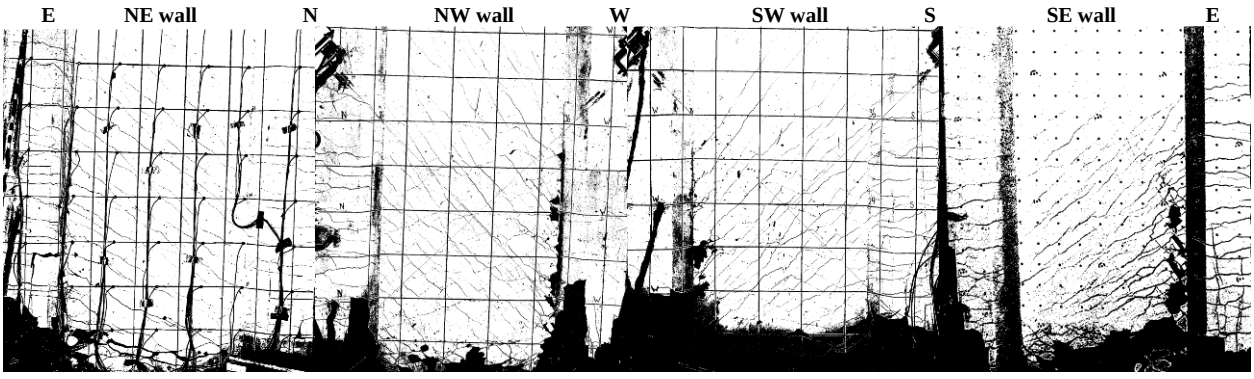

Figure 7. BPT web crushing failure at $\mu_\Delta = 6$ loading toward B.

The hysteretic force-displacement response of the DPT and BPT units along their principal axes is shown in Fig. 8 and Fig. 9, respectively. The hysteretic loops of the BPT unit at $\mu_\Delta = 4$ are isolated and shown in Fig. 10, which shows the distinct feature from unloading effects while transitioning from G to H in the longitudinal direction and D to E in the transverse direction. This phenomenon illustrates the interactions of the flexural behavior of the test unit under biaxial loading, which leads to what are considered important effects of unloading and reloading of the longitudinal steel and the change of the stress state in the compression zone.

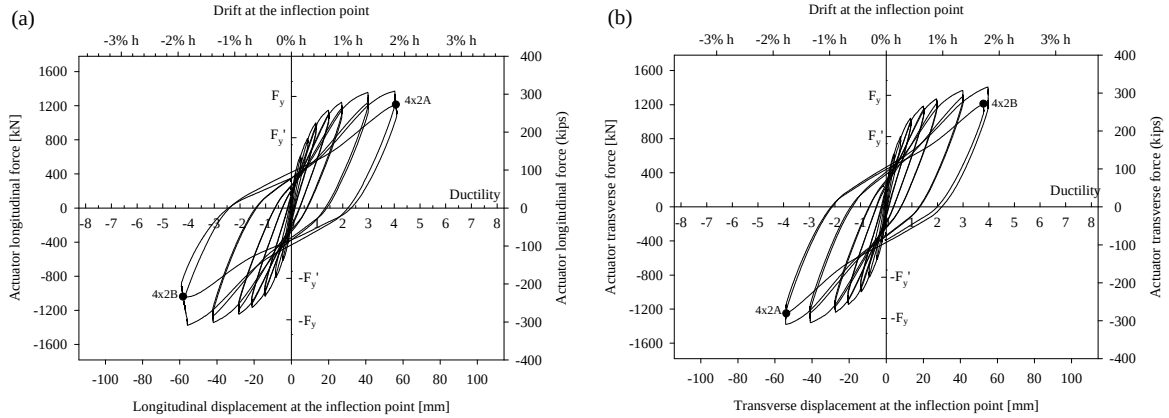

Figure 8. Hysteretic loops of DPT: (a) longitudinal axis and (b) transverse axis.

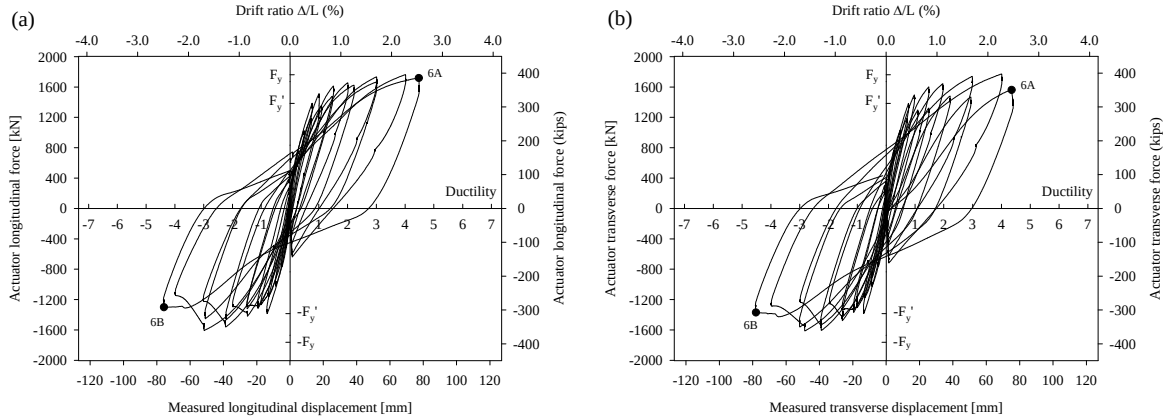

Figure 9. Hysteretic loops of BPT: (a) longitudinal axis and (b) transverse axis.

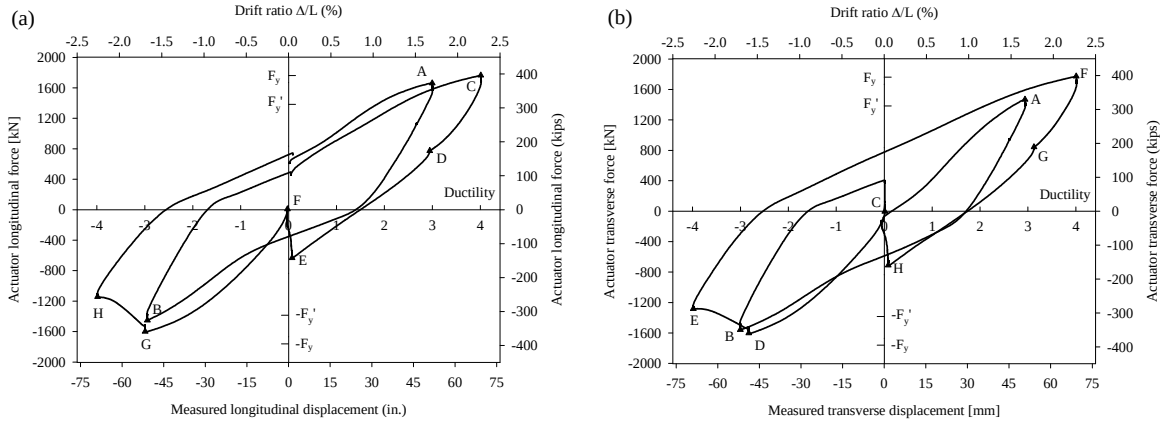

Figure 10. Hysteretic loops of BPT at $\mu_\Delta = 4$: (a) longitudinal axis and (b) transverse axis.

Discussion

Fig. 11 compares the force-displacement envelopes of BPT in different directions. It is interesting to note that the behavior of the test unit in the sweeping diagonal direction is close to that of the principal directions instead of the straight diagonal directions. The coupling between the two orthogonal directions decreases the stiffness in the sweeping diagonal direction. In comparison, the loading along the other directions passes through the centroid of the cross section and no coupling exists.

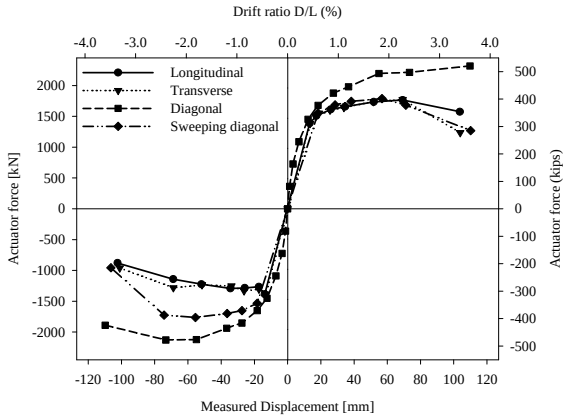

Figure 11. Comparison of the BPT force-displacement envelopes in different directions.

The shear stiffness degradation and the energy dissipating capacity of the inelastic shear mechanism of the test units under various loading patterns are of interest in this study. The displacement ductility limit of the hollow piers before web crushing failure is directly related to those two factors. Fig. 12 and 13 show the hysteretic loops of both test units for flexure and shear deformations, respectively. It can be seen that flexure (Fig. 12(a) and Fig. 13(a)) dominates the force-displacement behavior of both test units, while comparison of Fig. 12(b) and Fig. 13(b) indicates that the DPT unit exhibited larger inelastic shear deformations and energy dissipating capacity than the BPT unit.

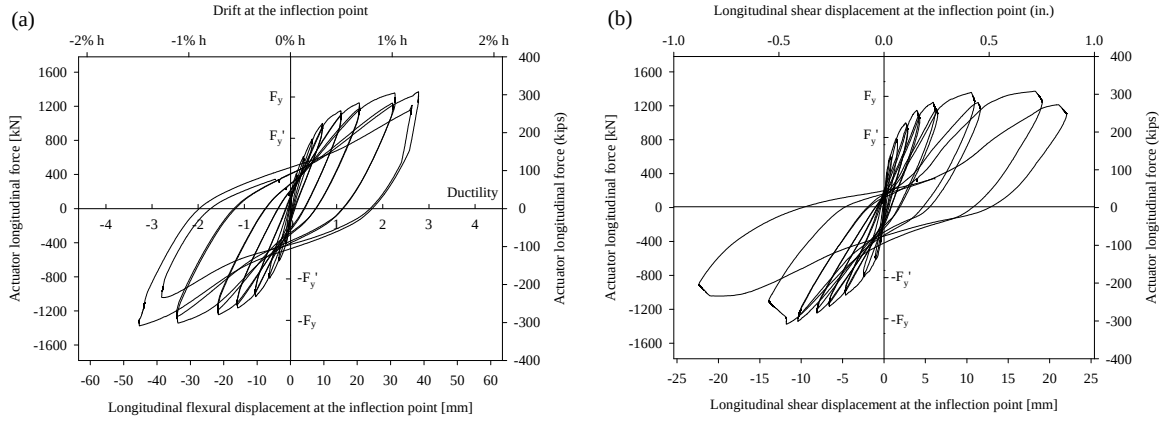

Figure 12. Hysteretic loops of DPT in (a) flexure and (b) shear.

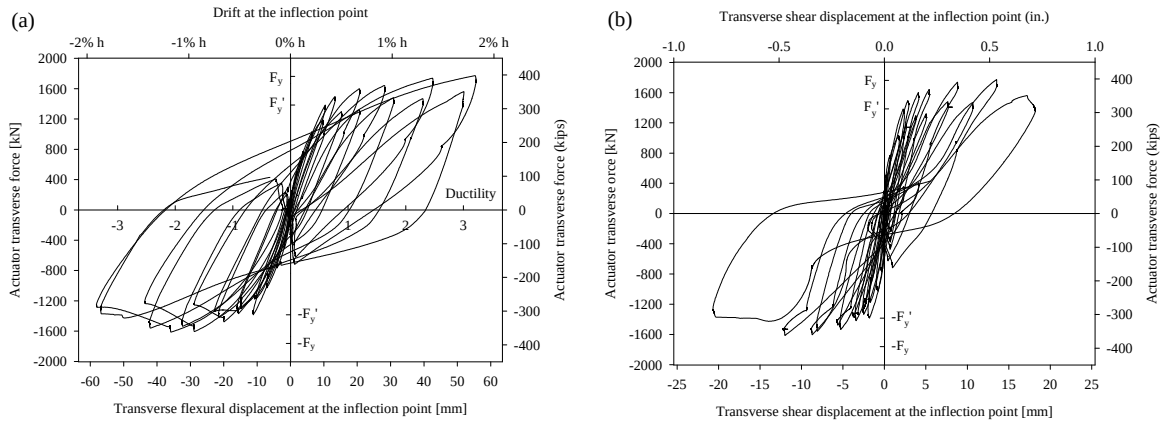

Figure 13. Hysteretic loops of BPT in (a) flexure and (b) shear.

To study the shear stiffness degradation of the DPT, a linear regression analysis was conducted on the unloading curves of the shear hysteretic loops. The unloading stiffness degradation of the DPT against displacement ductility is shown in Fig. 14(a). It is noteworthy to see that the damage degradation from the first loading peak (point A) with respect to the second loading peak (point B) progressively decreases, indicating overall damage to the structure.. For the BPT, the "butterfly" loading pattern disturbed the unloading scheme of the test units and the unloading stiffness is difficult to evaluate. Therefore, the degradation of the secant stiffness was studied since plastic shear deformations were small. The secant stiffness degradation of BPT is shown in Fig. 14(b). Of interest here is the fact that the degradation follows a quadratic trend, compared to the linear degradation than is seen in structural walls subjected to in-plane shear demands (Hines and Seible 2004, Liu 2009b). More discussion on this observation follows.

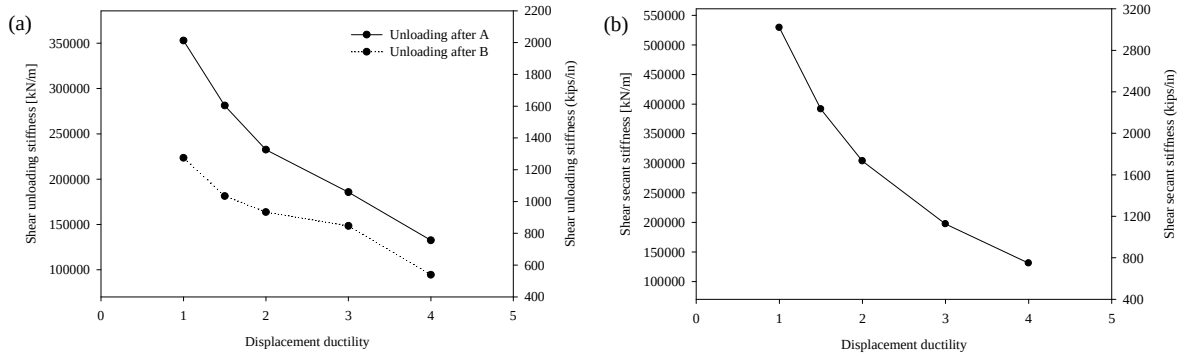

Figure 14. Multidirectional loading effects: (a) Shear unloading stiffness degradation of DPT in longitudinal direction, and (b) Shear secant stiffness degradation of BPT in transverse direction.

Hines et al. (Hines 2001) tested a single cantilever wall (Unit 3A) with the same cross section, steel reinforcement, and aspect ratio as one sides of the pier units in this program. Fig. 15 shows the global and the shear hysteretic loops of Unit 3A. A comparison of the shear hysteretic loops indicates that Unit 3A exhibited less shear stiffness degradation and better inelastic shear behavior than the pier units in this program, for which the mixed flexure-shear cracking under multi-directional loading caused rapid shear stiffness degradation. The shear dissipating energy of both piers along principal directions is compared with that of Unit 3A in Fig. 16. It can be seen that BPT has less shear energy dissipating capacity than DPT and that

both pier tests dissipated much less energy compared to the twice of the single wall test. The linear energy dissipation of the in-plane loaded wall compared to the quadratic degradation of the piers can also be noted.

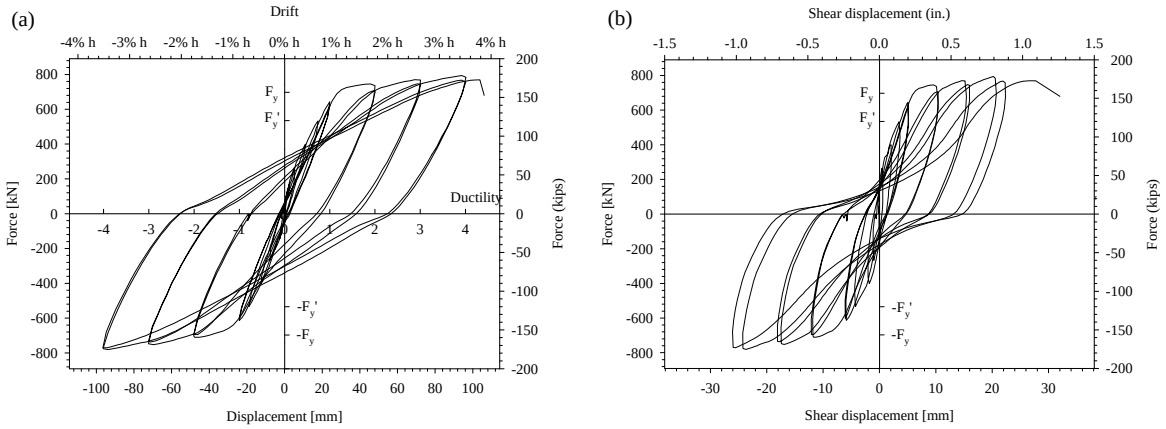

Figure 15. Hysteretic loops of Unit 3A (a) Global behavior (b) Shear behavior (Hines 2004).

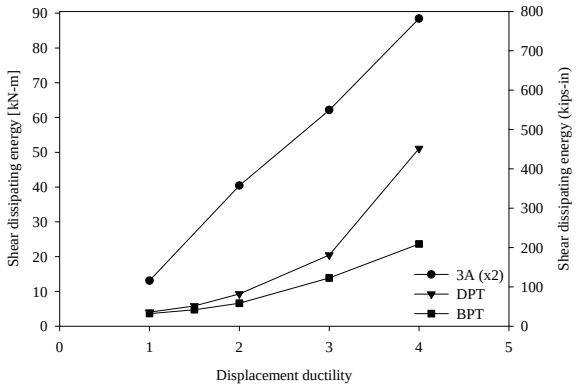

Figure 16. Comparison of shear dissipating energy of pier tests and single wall test.

Conclusions

The effect of multi-directional loading effect on the inelastic web crushing capacity of HSC hollow rectangular bridge piers was experimentally investigated through tests on two 1/4-scale units subjected to diagonal and multi-axial cyclic loading. Results to date have confirmed some of the advantages hypothesized for using HSC but have also brought forth important issues in establishing performance limits to inelastic web crushing in walls under three-dimensional shear demands. The following conclusions are offered based on the noted results and findings to date.

1. Both pier test units exhibited a stable ductile response up to moderate ductility levels before experiencing a web crushing shear failure. The three dimensional force-resisting mechanism provided by the integrated response of the boundary elements to resist flexure and the walls to resist shear was efficient and can be relied upon for new designs.
2. The effect of high-strength-concrete (HSC) in delaying the web-crushing shear failure in

the BPT compared to the DPT was verified even when the wall assembly was loaded under more severe multi-directional demands.

3. The BPT unit exhibited less inelastic shear deformation and more damage due to the application of HSC and the multi-directional loading pattern compared to the DPT unit. Therefore, the use of HSC to increase the ductility level was impaired by the severe biaxial loading pattern and the higher damage susceptibility of HSC.
4. Compared to a prior single wall test by Hines (2001), both pier test units exhibited rapid shear stiffness degradation, which is attributed to the damage accumulation under multi-directional loading and the lower fracture toughness of HSC.

Acknowledgements

The research described in this paper was carried out under funding from the National Science Foundation under Grant No. CMS-0530634. The authors thank the staff and students of the University of Minnesota's NEES-MAST laboratory where the reported tests were conducted.

References

Bousias, S. N., Verzeletti, G., Fardis, M. N., and Guitierrez, E., 1995. Load-Path Effects in Column Biaxial Bending and Axial Force, *Journal of Engineering Mechanics*, 125 (5), pp. 596-605.

Hines, E. M., Dazio, A., and Seible, F., 2001. Seismic Performance of Hollow Rectangular Reinforced Concrete Piers with Highly-Confined Corner Elements – Phase III: Web Crushing Tests, *SSRP Report No. 2001/27*, University of California, San Diego, La Jolla, CA, 2001, 239 pp.

Hines, E. M. and Seible, F., 2004. Web Crushing of Hollow Rectangular Bridge Piers, *ACI Structural Journal*, 101 (4), 569-579.

Hines, E. M., Dazio, A., and Seible, F., 2006. Structural Testing of New East Bay Skyway Piers, *ACI Structural Journal*, 103 (1), pp. 103-112.

Liu, X., Burgueño, R., Egleston, E., and Hines, E. M., 2009a. Inelastic Web Crushing Performance Limits of High-Strength-Concrete Structural Wall – Single wall Test Program, *Report No. CEE-RR – 2009/03*, Michigan State University, 2009, 281 pp.

Liu, X., Burgueño, R., Egleston, E., and Hines, E. M., 2009b. Inelastic Web Crushing Performance Limits of High-Strength-Concrete Structural Wall – Wall-Assembly Test Program, *Report No. CEE-RR – 2009/06*, Michigan State University, 2009, 219 pp.

Maria, H. S., Wood, S. L., and Breen, J. E., 2006. Behavior of Hollow, Rectangular Reinforced Concrete Piers Subjected to Biaxial Loading, *ACI Structural Journal*, 103 (3), pp. 390-398.

Mo, Y. L., Wong, D. C., and Maekawa, K., 2003. Seismic Performance of Hollow Bridge Columns, *ACI Structural Journal*, 100 (3), pp. 337-348.

Oesterle, R. G., Ariztizabal-Ochoa, J. D., Fiorato, A. E., Russell, H. G., and Corley, W. G., 1979. Earthquake Resistant Structural walls – Tests of Isolated Walls, Phase II, *NSF Report ENV77-15333*, Portland Cement Association, Skokie, IL, 331 pp.

Paulay, T., and Priestley, M. J. N., 1992. *Seismic Design of Reinforced Concrete and Masonry Buildings*, Wiley Interscience, New York, 768 pp.

Takizawa, H. and Aoyama, H., 1976. Biaxial Effects in Modelling Earthquake Response of R/C Structures, *Earthquake Engineering and Structural Dynamics*, Vol. 4 (6), pp. 523-552.

Vallenas, J. M., Bertero, V. V., Popov, E. P., 1979. Hysteretic Behavior of Reinforced Concrete Structural Walls, University of California, *Report No. UCB/EERC-79/20*, Berkeley, CA, 234 pp.

Wong, Y., Paulay, T., and Priestley, M. J., 1993. Response of Circular Reinforced Concrete Columns to Multi-Directional Seismic Attack, 90 (2), pp. 180-191.